Chapter 8

Spatiotemporal Investigation of Phosphorylation Events During Cell Cycle Progression

Lilia Gheghiani and Olivier Gavet

Abstract

Polo-like kinase 1 (Plk1) is an essential kinase for mitotic commitment and progression through mitosis. In contrast to its well characterized roles during mitosis, the precise molecular events controlled by Plk1 during G2/M progression and their spatiotemporal regulation are still poorly elucidated. We recently investigated Plk1-dependent regulation of Cdc25C phosphatase, an activator of the master mitotic driver Cyclin B1-Cdk1. To this end, we generated a genetically encoded FRET (Förster Resonance Energy Transfer)-based Cdc25C phosphorylation biosensor to observe Cdc25 spatiotemporal phosphorylation during cell cycle progression in live single cell assays. Because this approach proved to be powerful, we provide here guidelines for the development of biosensors for any phosphorylation site of interest.

Key words Phosphorylation, Kinase, Biosensor, FRET, Time-lapse imaging, Fluorescence microscopy

1 Introduction

1.1 Protein Phosphorylation

Protein phosphorylation is the most common post-translational modification used to finely tune any cellular process and is therefore a master regulatory mechanism for the maintenance of cell homeostasis. Reversible phosphorylation/dephosphorylation events are often associated with a switch in the active state of target proteins and reflect modifications over time by opposite protein kinase and phosphatase activities. Transcriptome and proteome analyses have revealed that most human diseases are associated with the deregulation of kinase and/or phosphatase expression levels. However, we frequently ignore the extent to which this will modify the spatiotemporal regulation of their enzymatic activities and as a consequence the phosphorylation states of their target proteins. A panel of elegant and powerful experimental approaches has recently emerged to identify target phosphorylation sites on a given protein and upstream kinase(s) and phosphatase(s) activities, including large-scale phosphoproteomic analyses, live-cell RNAi

Amanda S. Coutts and Louise Weston (eds.), *Cell Cycle Oscillators: Methods and Protocols*, Methods in Molecular Biology, vol. 1342, DOI 10.1007/978-1-4939-2957-3_8,

screens of protein kinase and phosphatase libraries and ATP analog labeling of protein kinase substrates [1–3]. Nevertheless, deciphering spatiotemporal regulation of any phosphorylation event, i.e. when and where this post-translational modification is initiated and/or turned off, is still a major challenge in cell biology. This is best illustrated by our weak understanding of how different signaling pathways are coordinated together into a coherent whole in space and time to control main cell cycle transitions as well as their spatiotemporal deregulations in tumoral conditions.

One popular approach, following the identification of a specific phosphorylation site, is the development of a corresponding phospho-specific antibody for qualitative and/or semi-quantitative immunofluorescence (IF) microscopy. In fact, IF is particularly powerful to detect any local phosphorylation of even a small fraction of a given protein. This will provide spatiotemporal information if the corresponding protein is concentrated at a particular subcellular location and if morphological landmarks are available. As an example, activating phosphorylation (T210P) of the mitotic Polo-like kinase 1 (Plk1) at the centrosome can be recorded during well identified mitotic stages (from prophase to anaphase) [4]. Conversely, phosphorylation states of diffusible proteins and/or absence of morphological landmarks are strongly limiting conditions. Accordingly, the activating phosphorylation kinetics of the diffusible cytoplasmic Plk1 pool during G2 phase progression has been under debate [4–6]. Also, IF detection of local phosphorylation events on fixed cells can be poorly informative of the underlying regulatory mechanisms taking place. In fact, local detection of active (T210P) Plk1 at the centrosome, as mentioned above, could reflect several scenarios: (1) its activation process could be restricted to this particular subcellular location, (2) following cytoplasmic activation, active Plk1 kinase could be recruited to the centrosome through unmasking of its anchoring domain (Polo-Box Domain), (3) initial activation of centromeric and cytoplasmic pools could be concurrent but the detection of cytoplasmic active Plk1 is limited by its diffusible distribution. FRET-based phosphorylation biosensors offer a powerful alternative to access the spatiotemporal regulation of phosphorylation events in live single cell assays.

1.2 Polo-Like Kinase 1 and Mitotic Commitment

Plk1 is an essential mitotic kinase for several processes including mitotic entry, centrosome maturation, sister chromatid resolution, stable attachment of chromosomes to the spindle apparatus and cleavage furrow formation [7–9]. Consistent with its involvement in the control of mitotic commitment, direct regulators (including activating phosphatases Cdc25B & C and inhibitory kinases Wee1 & Myt1) of the master mitotic driver Cyclin B1-Cdk1 have been found to be phosphorylated, at least in vitro, by Plk1. While the biological significance of Plk1-dependent Myt1 and Cdc25B phosphorylation is waiting further investigation, Plk1 has been shown

to promote Wee1 degradation through beta-TrCP-dependent mechanisms during G2/M progression, although it is not yet known whether this event precedes or follows mitotic entry [10]. Also, several reports show that Plk1 (or Plx1, *Xenopus laevis* homolog) stimulates Cdc25C (XCdc25C) phosphatase activity in vitro, by which it could promote Cyclin B1-Cdk1 initial activation and mitotic (meiotic) entry [11, 12]. Accordingly, hyperphosphorylation of Cdc25C during G2/M progression is sensitive to Plk1 inhibition. However, the different Plk1-dependent phosphorylation sites on Cdc25C and their spatiotemporal regulation during G2/M transition have been poorly characterized, strongly limiting our understanding of the relative importance of this regulatory mechanism for the control of mitotic commitment.

1.3 Plk1-Dependent Cdc25C Phosphorylation

We recently performed phosphoproteomic analysis to cover the whole Cdc25C protein sequence and identified eight Plk1-dependent phosphorylation sites, among them S38, 61 and 75 are fully conserved in vertebrates [6]. We generated a phospho-specific antibody against the S75 phosphosite which is surrounded by a canonical Plk1 consensus sequence and confirmed its Plk1-dependent phosphorylation during mitosis. Nevertheless, due to the diffusible cytoplasmic distribution of Cdc25C, we could not unambiguously determine when this phosphorylation event was initiated around the G2/M transition by IF, as discussed above. Instead, as described in the details of this chapter, we developed and optimized a FRET-based Cdc25C-S75 phosphorylation biosensor, which gave us access to its spatiotemporal regulation during cell cycle progression. We believe that this methodology could be broadly applied to investigate real-time regulation of any phosphorylation event following its previous identification by other experimental approaches.

1.4 Genetically Encoded Phosphorylation Biosensor

Genetically encoded FRET-based phosphorylation biosensors typically include a "sensor unit" which consists of a short phosphorylation sequence of interest (~10–20 amino acids) and a phosphorylation binding domain able to recognize this site in its phosphorylated state, both sandwiched between a pair of fluorescent proteins (usually CFP and YFP or their close derivatives). Conformational changes associated with the reversible phosphorylation of such biosensors affect the efficiency of non-radiative energy transfer between the donor (CFP) and the acceptor (YFP) fluorophores upon CFP excitation, which can be recorded in real time in live single cell assays. Efficient fluorescence resonance energy transfer between compatible fluorescent protein pairs is a function of the inverse sixth power of their absolute distance but is also strongly dependent on the relative orientation of their dipole moments. Optimization of these two parameters to improve the FRET dynamic range (sensitivity) of any biosensor can be a tedious process.

In order to override this main limitation, several FRET-dedicated vector libraries have recently emerged based on the use of differently connected circularly permutated forms of donor (CFP variant mTFP1) and/or acceptor (YFP variant Venus) fluorescent proteins to modulate their relative spatial orientation [13, 14]. Such libraries can also comprise short amino-acid sequences ("linkers") of different length between each fluorescent protein and the "sensor unit" to further modulate the orientation and/or absolute distance between them. From data currently available, it appears that using different circularly permutated forms is a more easy way to rapidly improve, as a first step, the dynamic range of any biosensor [13]. On the other hand, using linker random mutagenesis and large-scale (up to 1,00,000) bacterial colonies screening, Oliver Griesbeck's group recently selected calcium reporters exhibiting ratio changes of up to 1000 % in bacteria, demonstrating the potential to optimize linker sequences to generate highly sensitive biosensors [15].

Although commonly called "kinase biosensors," one should keep in mind that these sensors will, in most cases, report changes in the equilibrium between opposite kinase and phosphatase activities rather than modification of the kinase activity alone, i.e. when the phosphorylation of the target site becomes effective. As an example, this strategy proved to be powerful to decipher phosphorylation changes of Plk1-dependent kinetochore substrates during prometaphase to metaphase transition, which are finely tuned by the local recruitment of Plk1 and/or counteracting PP1 phosphatase [16]. A comprehensive list of phosphorylation site biosensors already available for several kinases (PKA, PKC, PKB/Akt, ERK, Aurora-B, CyclinB1-Cdk1, etc.) can be found at the following address: http://biosensor.dpb.carnegiescience.edu.

2 Materials

2.1 FRET-Dedicated Plasmid Library

We used a FRET-dedicated vector library previously developed by Carsten Schultz's group (EMBL, Germany; [13]). This library contains CFP variant mTurquoise as the fluorescent donor and YFP variant Venus or cp49Venus, cp157Venus, cp173Venus, cp229Venus as the fluorescent acceptors together with short linkers of different sizes (two, four, or eight amino acids). YPet fluorescent protein was also inserted as an alternative YFP variant acceptor [17] (Fig. 1a).

1. Cloning primers:

   FHA2 forward Primer 5′→3′ (**AgeI**) GCG **ACC GGT** AAG GGT AAT GGT AGG TTT TTA ACT

   FHA2 reverse Primer 5′→3′ (**MluI EcorI**) GCG **ACG CGT GAA TTC** TAA CTT TTT CAC CAA ATC TTT TTC T

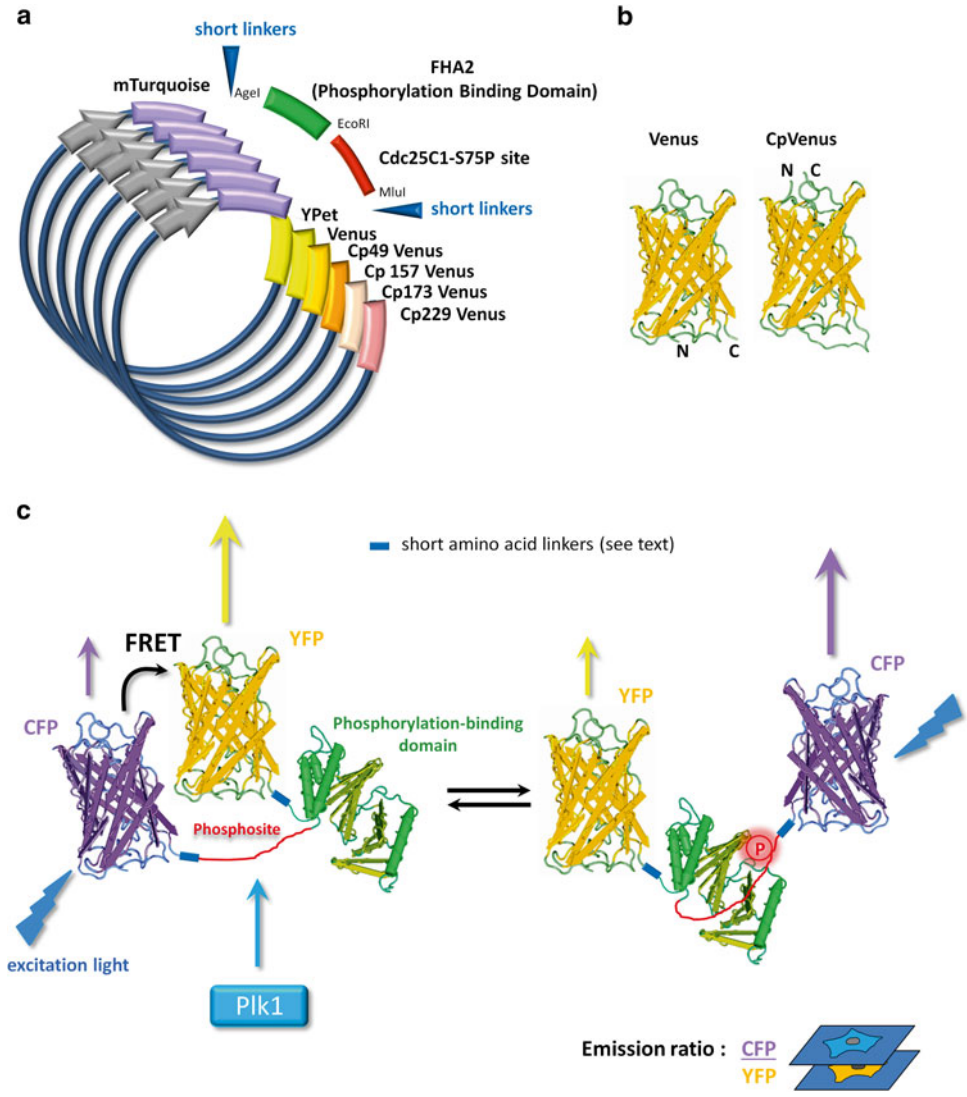

Fig. 1 (**a**) FRET-dedicated vector library containing fluorescent CFP donor (Turquoise), YFP acceptors (Ypet, Venus, and cpVenus) and short linker sequences (2, 4, or 8 amino acids) [13]. Restriction sites used for cloning are also indicated. (**b**) Schematic representation of differentially connected Venus and cpVenus. (**c**) General scheme of the FRET-based phosphorylation biosensor. Phosphorylation of a specific target residue induces its recognition by the phosphorylation binding domain and a conformational change occurs, affecting the efficiency of energy transfer between fluorescent donor and acceptor proteins

2. Restriction enzymes : AgeI (**ACC GGT**), MluI (**ACG CGT**), EcoRI (**GAA TTC**)
3. Vent DNA polymerase
4. T4 DNA ligase
5. Alkaline phosphatase, Calf Intestinal (CIP)

6. Competent bacteria: subcloning efficiency DH5a
7. LB-Kanamycin agar plates
8. Low melting point agarose

2.2 Cell Culture and Transfection

1. Homo sapiens cervix epithelial HeLa cell line.
2. Dulbecco's Modified Eagle's Medium supplemented with 10 % fetal bovine serum (FBS), 2 mM Glutamine, 100 U/ml penicillin, and 100 μg/ml streptomycin.
3. Fibronectin from human plasma.
4. JetPrime transfection reagent.
5. Nocodazole.
6. 24 glass-bottom well plate or 35-mm glass-bottom imaging dishes.
7. Phenol red free Dulbecco's Modified Eagle or Liebowitz-15 (L15) medium supplemented with 1 % fetal bovine serum (FBS) and 2 mM Glutamine.

2.3 Wide-Field Imaging

1. The imaging setup uses an inverted motorized microscope (Leica DMI6000) equipped with temperature and CO_2-humidified controller systems, adaptive focus control, fast emission filter wheel lambda 10-3 (Sutter Instruments, Novato, CA, USA), electron multiplier charge-coupled device camera (Evolve 512; Photometrics), HCX PL APO 40×/1.30 Oil objective and multi LED illumination system (spectra X-light engine, Lumencor). High NA oil immersion objectives are preferred due to their high light collecting efficiency.
2. Emission filters ET480/40, ET535/30m and CFP/YFP dichroic mirror 51017bs (Chroma Technology Corp., Brattleboro, VT, USA).

2.4 Image Acquisition

1. Wide-field imaging setup is controlled by Metamorph software (Molecular Devices, Sunnyvale, CA).

2.5 Image Analysis

1. Image analysis is performed using ImageJ software (NIH).

3 Methods

3.1 Design Intramolecular Cdc25C-S75 Phosphorylation Biosensors

We used AgeI and MluI sites inserted between donor and acceptor fluorescent protein sequences for subsequent cloning as described in Piljic et al. [13] (Fig. 1a).

1. Digest the CFP and YFP containing vectors with AgeI and MluI restriction enzymes, and dephosphorylate them with alkaline phosphatase enzyme.

2. Perform PCR amplification of the FHA2 phosphorylation binding domain sequence from yeast ScRad53p with 5′ and 3′ primers containing AgeI and MluI&EcoRI restriction sequences (*see* **Note 1**).
3. Digest the PCR product with AgeI and MluI restriction enzymes.
4. Run digested PCR products on a 0.5 % low melting point agarose gel.
5. Purify the digested product from the gel using standard protocols.
6. Insert the FHA2 fragment in the vector backbones using vector:insert molar ratios between 1:3 and 1:10 and T4 DNA ligase.
7. Transform the reaction mix into competent bacteria using standard protocols.
8. Plate the transformed bacteria on LB-Kanamycin agar plates.
9. Pick up individual colonies and inoculate LB medium containing Kanamycin antibiotic.
10. Prepare plasmid DNA using a plasmid miniprep kit.
11. Check plasmid constructs by DNA sequencing.
12. Design primers for the phosphorylation site of interest. We used complementary nucleotide sequences coding for the following peptide NH_2-G-G-A-P-K-R-C-L-L-**T**-N-L-I-COOH. This sequence is from HsCdc25C, residues 66–78, with Ser75 replaced with Thr and an Ile amino-acid inserted at +3 position in order to optimize FHA2 binding (*see* **Note 1**).
13. Anneal complementary oligonucleotides exhibiting overlapping 5′ ends for EcoRI & MluI restriction sites according to standard protocols.
14. Linearize the vector backbones containing the FHA2 domain with both EcoRI and MluI restriction enzymes. Do not dephosphorylate the vectors.
15. Subclone the annealed oligonucleotides into the different vector backbones.
16. Transform the different constructs into competent bacteria.
17. Plate the transformed bacteria on LB-Kanamycin agar plates.
18. Pick up individual colonies and inoculate LB medium containing Kanamycin antibiotic.
19. Prepare plasmid DNA using a plasmid miniprep kit (Plasmid DNA for transfection into mammalian cells should be preferentially prepared using commercial endotoxin-free MiniPrep and/or MaxiPrep kits to limit cell toxicity).
20. Check plasmid constructs by DNA sequencing.
21. If required, a protein-targeting domain can be inserted into the biosensor constructs (*see* **Note 2**).

3.2 Cell Culture

1. Culture human cervix carcinoma HeLa cells in Dulbecco's Modified Eagle Medium supplemented with 10 % fetal bovine serum (FBS), 2 mM Glutamine, 100 U/ml penicillin, 100 µg/ml streptomycin at 37 °C with 5 % CO_2.
2. Seed cells on a 24-well glass bottom plate or on a 35 mm glass bottom dish pre-coated with fibronectin (1 µg/cm^2) for 1–2 h at a density of 50,000 cells per well or 200,000 cells per dish, respectively.

3.3 Cell Transfection and Synchronization

The day after seeding, transfection of the different biosensor constructs can be carried out with a transfection reagent such as JetPrime, according to the manufacturer's recommendations. In brief:

1. Add 4 µl of JetPrime reagent and 1 µg of the plasmid construct to 200 µl of JetPrime buffer.
2. Mix gently by tapping and further incubate for 15 min at room temperature.
3. Add the mixture to the cells cultured in medium without antibiotics and incubate for 4 h.
4. Replace the culture medium and add thymidine 2.5 mM for ~15–20 h to synchronize the cells in S phase.
5. Add the microtubule depolymerizing drug Nocodazole (100 nM) 6 h post-thymidine release (G2 phase) for ~3–5 h to enrich for mitotic cells.

3.4 Screening

In order to determine the FRET dynamic range of each biosensor between phosphorylated and dephosphorylated states, we analyzed the average CFP/YFP emission ratio values in interphase (S phase) and mitotic synchronized cells. In fact, Plk1 protein is expressed from G2 phase onset and reaches a maximum activity level during mitosis [18].

1. Image acquisition is performed in CO_2-independent L15 culture medium (*see* **Note 3**).
2. Using the eyepieces, quickly select in each well several stage positions with healthy cells exhibiting appropriate fluorescent levels (*see* **Note 4**).
3. Avoid unnecessary exposure of the cells to excitation light.
4. Acquire CFPex/CFPem and CFPex/YFPem snapshot images of the different positions using the same exposure time (usually between 30 and 200 ms, depending on the biosensor expression level, illumination power and camera sensitivity (*see* **Note 5**)).

3.5 Data Analyses

All image analysis is performed using ImageJ software.

1. Draw a region of interest (ROI) around each fluorescent cell of interest.

2. Check that the cell remains inside the ROI during time-lapse experiments.
3. Save ROI-1 using ROI manager tool.
4. Choose a close region devoid of cells for fluorescence background correction.
5. Save ROI-2 using ROI manager tool.
6. Measure area, average and sum intensities of each ROI.
7. Export values to Excel or Prism software.
8. FRET ratio measurement is performed using the following formulae:
   (a) Whole cell signal = sum of the intensity of the pixels for ROI-1.
   (b) Background signal = average value per pixel for the region selected just beside the cell of interest (ROI-2).
   (c) Whole-cell signal corrected = whole cell signal – ((area selected=number of pixels for ROI-1) × background signal).
   (d) CFP/YFP emission ratio = whole cell CFP signal corrected/whole cell YFP signal corrected.
9. Determine the average CFP/YFP emission ratio from several cells expressing any biosensor construct in both control (S phase) and stimulation conditions (M-phase arrested cells).
10. Compare the average FRET (CFP/YFP emission ratio) dynamic range between both conditions for each biosensor construct (*see* **Note 6**).

3.6 Controls

Following the identification of the Cdc25C-S75 biosensor construct exhibiting the highest dynamic range between interphase and mitotic cells, we performed several control experiments.

1. An inactive biosensor mutated on its internal phosphorylation site (for example, to a non-phosphorylatable Ala residue) is used to confirm that FRET changes are dependent on its phosphorylation level and are not a consequence of morphological changes during the cell division process or due to differential photobleaching of the donor and/or acceptor fluorescent proteins during recording.
2. To confirm biosensor sensitivity to a specific kinase activity of interest, one could inhibit its expression by an RNA interference approach. Alternatively, we analyzed FRET changes in mitotic arrested cells following dose-dependent inhibition of Plk1 kinase using different selective compounds (BI 2536, BI6727).
3. Because Plk1 and checkpoint kinase Mps1 share closely related target sites, we also checked that the Cdc25C-S75 phosphorylation biosensor is insensitive to Mps1 inhibition

(Reversine + MG132). Note that Proteasome inhibitor (MG132) is required to prevent premature mitotic exit following Mps1 inhibition.

4. Finally, using a broad PP1 & PP2A inhibitor (okadaic acid, 500 nM) added on mitotic cells, we found that the raise of Cdc25C-S75 biosensor phosphorylation during mitosis is not due to the inactivation of counteracting phosphatase(s).

3.7 Generation of Biosensor Stably Expressing Cells

To facilitate subsequent microscopy analyses, we generated HeLa cell populations stably expressing the biosensor of interest:

1. Subclone the biosensor sequence into a vector containing an antibiotic resistance gene (*see* **Note 7**).
2. Transfect cells using the same protocol as for transient expression.
3. 2 days after transfection, select cells by the addition of the appropriate antibiotic into the culture medium.
4. Optional: transfected fluorescent cells can be sorted out at this time by flow cytometry.
5. Change the culture medium containing the antibiotic every 2–3 days to maintain selection pressure.
6. Clones of resistant cells can be observed after ~2 weeks of selection.
7. After 3–4 weeks, all clones are collected by trypsination and stably expressing cells are sorted by flow cytometry to generate a homogeneous cell population exhibiting equivalent fluorescent (YFP and/or CFP) expression levels (*see* **Note 8**).

3.8 Time-Lapse Experiments

1. For time-lapse experiments on a multi-well plate, a 40× air objective should be preferentially used to avoid air bubble formation during recording. Conversely, multi-position recording (up to ~40, depending on their absolute distance, exposure times and time-lapse intervals) of biosensor-expressing cells can be performed in a 35 mm dish using an oil objective at around 1 image/min for ~3–4 h duration or at 1 image/3 min for 10–24 h without cell phototoxicity (*see* **Note 9**).
2. Perform time-lapse image analysis as previously described in Subheading 3.5.
3. Plot CFP/YFP emission ratio values over time. To facilitate the comparison of different cells, the emission ratio can be expressed as a percentage of the initial value (Fig. 2a).
4. Pseudo-color Intensity-Modulated Display (IMD) representation of emission ratio values over time is performed using Metamorph Software. We selected the 8-color hues option with 32 intensities displayed for each color ranking from dark to bright (Fig. 2b). The max and min ratio values are generally

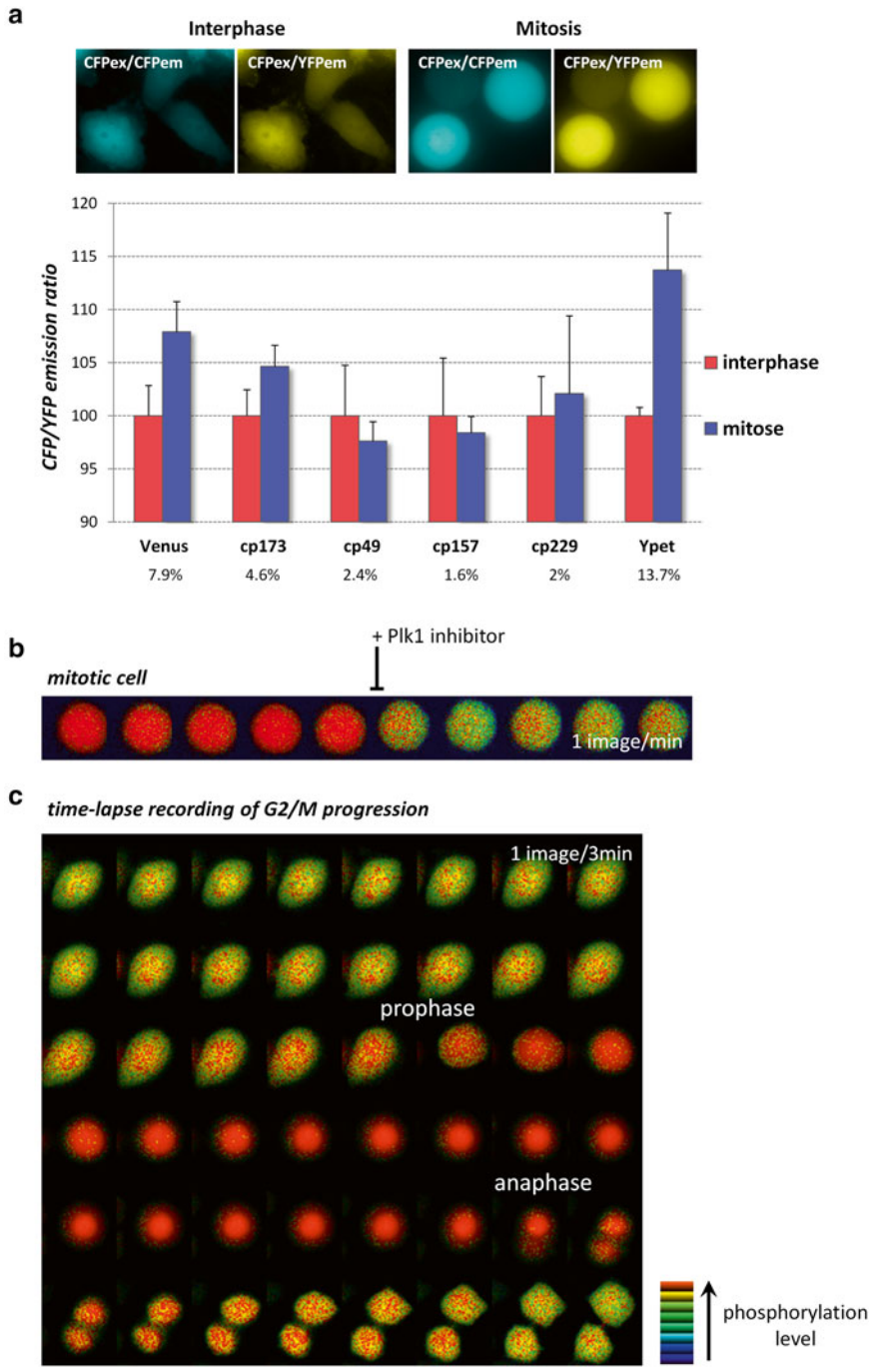

Fig. 2 (**a**) HeLa cells were transfected with the Cdc25C-S75 biosensor constructs containing different YFP acceptor fluorescent proteins as indicated. Transfected cells were either synchronized in interphase (S) or mitosis before CFPex/CFPem and CFPex/YFPem imaging. The average CFP/YFP emission ratio for each biosensor construct in both experimental conditions is displayed. The YPet-based Cdc25C-S75 biosensor exhibited the highest dynamic range and was used for subsequent experiments. Note that a secondary screen can be performed using amino-acid linkers of different sizes. (**b**) Cdc25C-S75 biosensor-expressing cells in mitosis were treated with a Plk1 inhibitor (BI2536 200 nM) (1 image/min). (**c**) Cdc25C-S75 biosensor-expressing cells were recorded during cell cycle progression (1 image/3 min)

fixed manually in a trial-and-error approach. The color intensities displayed for each hue are then determined automatically by the software [19].

4 Notes

1. Previous phosphoproteomics analyses revealed that recognition of Plk1 target sites is mostly based on adjacent N-terminal positions of phosphorylated serine/threonine residues [3]. In order to preserve the Plk1 specificity to the inserted Cdc25C-S75 phosphorylation peptide, we used the FHA2 domain of scRad53p as a phosphorylation-binding domain in our biosensor constructs. In fact, the FHA domains (denoted FHA1 and FHA2) exhibit amino-acid preferences at the three positions immediately C-terminal to the pT/pS, particularly at the +3 position (Asp residue for FHA1 and Ile for FHA2) [20]. Accordingly, the +3 position in the Cdc25C-S75 phosphorylation peptide was replaced by an Ile residue. Note also that the choice of the phosphorylation-binding domain will affect to a certain extent the dephosphorylation of biosensors and the FRET dynamics recorded. As an example, the dissociation constants of FHA1 and FHA2 domains for their respective optimal peptides are 530 nM and 10 μM [20, 21].
2. If the phosphorylation of a given substrate is taking place at a particular subcellular location or if one wants to investigate temporal phosphorylation/dephosphorylation kinetics at this place, insertion of a protein-targeting domain into the biosensor constructs will facilitate subsequent recording and image analyses. Several examples have been previously described including plasma membrane [22], nuclear or cytoplasmic [23], centrosome [24], chromatin [25] and inner centromere or kinetochore [26] targeting domains.
3. We used CO_2-dependent or -independent growth medium without phenol-red such as Dulbecco's Modified Eagle or Liebowitz-15 (L15) medium, respectively, for microscopy imaging. L-15 exhibited a lower auto-fluorescence level and was preferable due to the higher signal-to-noise ratio during short-term experiments. Conversely, we used Dulbecco's Modified Eagle medium and a CO_2-humidified controller system to prevent any evaporation during long-term (>20 h) experiments.
4. It is important to empirically select healthy and well adherent cells exhibiting appropriate expression levels of fluorescent biosensors. In indeed, a weak expression level will lead to a low signal-to-noise ratio. Conversely, high expression levels could affect cell properties and/or viability. Also, weakly adherent

cells have a tendency to round up and re-adhere over the time course of the experiment, which could affect the emission ratio baseline.

5. Different illumination sources can be used for FRET measurements. Whereas Xenon lamps are, in our hands, inappropriate for efficient CFP excitation, Mercury or metal-halide arc bulbs work quite well. Neutral density filters should be used to attenuate illumination power and to avoid photobleaching of the donor and/or acceptor fluorescent proteins, which will affect the emission ratio measurements. Also, we strongly recommend to insert UV filters (>400 nm long pass) in both epi- and trans-illumination light paths to limit phototoxicity. Finally, we recently used LED-based CFP excitation, which is superior in terms of light power stability for time-lapse experiments and further limits UV exposure. Several companies provide single- or multi-wavelength LED systems (for example, CoolLED, Lumencor).
6. Several screening approaches have been previously described to select phosphorylation biosensors with higher FRET dynamics between the control and stimulation conditions, including emission spectrum analysis of biosensor transfected cell extracts by a spectrofluorometer [22], fluorescence monitoring of biosensor library transfected cells in 96-well plates using a plate reader fluorometer [14] and large-scale screening of bacteria colonies co-expressing phosphorylation biosensors and the recombinant kinase of interest [27]. Nevertheless, because fluorescence properties and/or the dynamic range recorded by fluorescent microscopy could significantly differ, a secondary screen performed through live single cell assays is still required.
7. We used commercial mammalian pIRES expression vectors which allow co-expression of the biosensor of interest and the antibiotic resistance gene from the same bicistronic mRNA transcript. This significantly reduced the selection of false-positive colonies that only exhibit antibiotic resistance.
8. Using the same protocol, one could generate cell populations stably co-expressing the biosensor of interest and a RFP-fused cell cycle progression marker (PCNA, DNA ligase I, Cyclin B1, etc.). Red fluorescent proteins (such as mCherry and mRuby) will not interfere with the recording of CFP & YFP emission signals.
9. Focus drift is a frequent problem in video-microscopy, even when using automatic focus control systems that are generally based on infrared light reflection from the dish or plate bottom. In practice, we found that glass bottom dishes are more suitable for autofocus systems than fluorescent compatible plastic bottom dishes. Also, the choice of the stage dish holder, which depends on the dish used, is essential to prevent any movement

that may occur during time-lapse multi-positioning recording. Examples can be found at http://www.biosciencetools.com/catalog/. Finally, the stage dish holder was permanently maintained at 37 °C, and following dish positioning, we routinely waited for at least 1 h before starting recording. We found that this set-up significantly limited initial focus drift.

References

1. Schmitz MH, Held M, Janssens V et al (2010) Live-cell imaging RNAi screen identifies PP2A-B55alpha and importin-beta1 as key mitotic exit regulators in human cells. Nat Cell Biol 12:886–893, doi: ncb2092 [pii] 10.1038/ncb2092
2. Blethrow JD, Glavy JS, Morgan DO, Shokat KM (2008) Covalent capture of kinase-specific phosphopeptides reveals Cdk1-cyclin B substrates. Proc Natl Acad Sci U S A 105:1442–1447. doi:10.1073/pnas.0708966105
3. Kettenbach AN, Schweppe DK, Faherty BK et al (2011) Quantitative phosphoproteomics identifies substrates and functional modules of Aurora and Polo-like kinase activities in mitotic cells. Sci Signal 4:rs5. doi:10.1126/scisignal.2001497
4. Macurek L, Lindqvist A, Lim D et al (2008) Polo-like kinase-1 is activated by aurora A to promote checkpoint recovery. Nature 455:119–123, doi: nature07185 [pii] 10.1038/nature07185
5. Seki A, Coppinger JA, Jang C-YY et al (2008) Bora and the kinase Aurora a cooperatively activate the kinase Plk1 and control mitotic entry. Science 320:1655–1658. doi:10.1126/science.1157425
6. Gheghiani L, Loew D, Lombard B et al (2015) Plk1 pool activation in late G2 sets up commitment to mitosis
7. Lénárt P, Petronczki M, Steegmaier M et al (2007) The small-molecule inhibitor BI 2536 reveals novel insights into mitotic roles of polo-like kinase 1. Curr Biol 17:304–315. doi:10.1016/j.cub.2006.12.046
8. Lane HA, Nigg EA (1996) Antibody microinjection reveals an essential role for human polo-like kinase 1 (Plk1) in the functional maturation of mitotic centrosomes. J Cell Biol 135:1701–1713
9. Petronczki M, Glotzer M, Kraut N, Peters J-M (2007) Polo-like kinase 1 triggers the initiation of cytokinesis in human cells by promoting recruitment of the RhoGEF Ect2 to the central spindle. Dev Cell 12:713–725. doi:10.1016/j.devcel.2007.03.013
10. Watanabe N, Arai H, Iwasaki J et al (2005) Cyclin-dependent kinase (CDK) phosphorylation destabilizes somatic Wee1 via multiple pathways. Proc Natl Acad Sci U S A 102:11663–11668
11. Roshak AK, Capper EA, Imburgia C et al (2000) The human polo-like kinase, PLK, regulates cdc2/cyclin B through phosphorylation and activation of the cdc25C phosphatase. Cell Signal 12:405–411, doi: S0898-6568(00)00080-2 [pii]
12. Kumagai A, Dunphy WG (1998) Purification and molecular cloning of Plx1, a Cdc25-regulatory kinase from Xenopus egg extracts. Science 273:1377–1380
13. Pilji A, Wilmanns M, Schultz C et al (2011) Rapid development of genetically encoded FRET reporters. ACS Chem Biol 6:685–691. doi:10.1021/cb100402n
14. Fritz RD, Letzelter M, Reimann A et al (2013) A versatile toolkit to produce sensitive FRET biosensors to visualize signaling in time and space. Sci Signal 6:rs12. doi:10.1126/scisignal.2004135
15. Thestrup T, Litzlbauer J, Bartholomäus I et al (2014) Optimized ratiometric calcium sensors for functional in vivo imaging of neurons and T lymphocytes. Nat Methods 11:175–182. doi:10.1038/nmeth.2773
16. Liu D, Davydenko O, Lampson MA (2012) Polo-like kinase-1 regulates kinetochore-microtubule dynamics and spindle checkpoint silencing. J Cell Biol 198:491–499. doi:10.1083/jcb.201205090
17. Nguyen AW, Daugherty PS (2005) Evolutionary optimization of fluorescent proteins for intracellular FRET. Nat Biotechnol 23:355–360. doi:10.1038/nbt1066
18. Golsteyn RM, Mundt KE, Fry AM, Nigg EA (1995) Cell cycle regulation of the activity and subcellular localization of Plk1, a human protein kinase implicated in mitotic spindle function. J Cell Biol 129:1617–1628
19. Tsien R, Harootunian A (1990) Practical design criteria for a dynamic ratio imaging sys-

tem. Cell Calcium 11:93–109. doi:10.1016/0143-4160(90)90063-Z

20. Durocher D, Taylor IA, Sarbassova D et al (2000) The molecular basis of FHA domain:phosphopeptide binding specificity and implications for phospho-dependent signaling mechanisms. Mol Cell 6:1169–1182
21. Violin JD, Zhang J, Tsien RY, Newton AC (2003) A genetically encoded fluorescent reporter reveals oscillatory phosphorylation by protein kinase C. J Cell Biol 161:899–909, doi: 10.1083/jcb.200302125 jcb.200302125 [pii]
22. Yoshizaki H, Ohba Y, Kurokawa K et al (2003) Activity of Rho-family GTPases during cell division as visualized with FRET-based probes. J Cell Biol 162:223–232, doi: 10.1083/jcb.200212049 jcb.200212049 [pii]
23. Gavet O, Pines J (2010) Activation of cyclin B1-Cdk1 synchronizes events in the nucleus and the cytoplasm at mitosis. J Cell Biol 189:247–259. doi:10.1083/jcb.200909144
24. Agircan FG, Schiebel E (2014) Sensors at centrosomes reveal determinants of local separase activity. PLoS Genet 10(10), e1004672. doi:10.1371/journal.pgen.1004672
25. Fuller BG, Lampson MA, Foley EA et al (2008) Midzone activation of aurora B in anaphase produces an intracellular phosphorylation gradient. Nature 453:1132–1136, doi: nature06923 [pii] 10.1038/nature06923
26. Liu D, Vader G, Vromans MJ et al (2009) Sensing chromosome bi-orientation by spatial separation of aurora B kinase from kinetochore substrates. Science 323:1350–1353. doi:10.1126/science.1167000
27. Belal ASF, Sell BR, Hoi H et al (2014) Optimization of a genetically encoded biosensor for cyclin B1-cyclin dependent kinase 1. Mol Biosyst 10:191–195. doi:10.1039/c3mb70402e